Evaluation of the Use of IRI Data to Estimate Bridge Dynamic Impact Factor (DIF)

Final Report
November 2022

BRIDGE ENGINEERING CENTER

About the Bridge Engineering Center

The mission of the Bridge Engineering Center (BEC) is to conduct research on bridge technologies to help bridge designers/owners design, build, and maintain long-lasting bridges.

About the Institute for Transportation

The mission of the Institute for Transportation (InTrans) at Iowa State University is to save lives and improve economic vitality through discovery, research innovation, outreach, and the implementation of bold ideas.

Iowa State University Nondiscrimination Statement

Disclaimer Notice

Iowa DOT Statements

Technical Report Documentation Page

1. Report No. InTrans Project 21-757	2. Government Accession No.	3. Recipient's Catalog No.
4. Title and Subtitle Evaluation of the Use of IRI Data to Estimate Bridge Dynamic Impact Factor (DIF)		**5. Report Date** November 2022
		6. Performing Organization Code
7. Author(s) Zhengyu Liu (orcid.org/0000-0002-7407-0912), Brent M. Phares (orcid.org/0000-0001-5894-4774), and Karthian R. Jadhav (orcid.org/0000-0001-6805-6578)		**8. Performing Organization Report No.** InTrans Project 21-757
9. Performing Organization Name and Address Bridge Engineering Center Iowa State University 2711 South Loop Drive, Suite 4700 Ames, IA 50010-8664		**10. Work Unit No. (TRAIS)**
		11. Contract or Grant No.
12. Sponsoring Organization Name and Address Iowa Department of Transportation 800 Lincoln Way Ames, IA 50010		**13. Type of Report and Period Covered** Final Report
		14. Sponsoring Agency Code

16. Abstract

The objectives of this project were to correlate international roughness index (IRI) data (which are widely collected and directly related to bridge deck roughness) to impact factors and develop a process for determining the impact factor to use for all bridges in Iowa.To achieve the project objectives, a sample of 20 bridges was selected for bridge monitoring to collect dynamic strain data.

To estimate the static strain data, the locally weighted scatterplot smoothing (LOWESS) function was used to smooth the dynamic strain time history. The dynamic impact factor (DIF) value was then calculated using maximum dynamic and static strain data. IRI data were extracted from PathWeb, a web-based application provided by the Iowa Department of Transportation (DOT) for all bridges considered in the field test program. Once the bridge was identified in PathWeb, the IRI data from four locations near each bridge deck approach were extracted and used to study the relationship between the IRI and DIF. Based on the results from this research, these were the key findings:

- The DIF value decreases as the bridge skew angle increases. Based on linear regression, the DIF value decreases about 0.037 to 0.043 per 10-degree increment of bridge skew.
- The DIF value decreases as the bridge deck condition index increases, meaning that the dynamic response is lower when the bridge deck condition is better.
- For bridges with zero skew, the DIF value increased by 0.006 per 100 in/mile increment of the IRI value.

According to the research findings, an equation was developed for the prediction of DIF on existing bridges with consideration of the bridge skew and the maximum IRI value near the bridge deck approach. Although the proposed equation was validated uing data from 13 bridges, the researchers recommend using the equation with the limitation that the actual bridge dynamic response could deviate ±10% from the equation predicted value.

17. Key Words bridge deck appoach—bridge DIF—dynamic impact factor—dynamic strain—IRI data—static strain		**18. Distribution Statement** No restrictions.	
19. Security Classification (of this report) Unclassified.	**20. Security Classification (of this page)** Unclassified.	**21. No. of Pages** 53	**22. Price** NA

Form DOT F 1700.7 (8-72)   **Reproduction of completed page authorized**

EVALUATION OF THE USE OF IRI DATA TO ESTIMATE BRIDGE DYNAMIC IMPACT FACTOR (DIF)

Final Report
November 2022

Principal Investigator
Brent M. Phares, Bridge Research Engineer
Bridge Engineering Center, Iowa State University

Research Assistants
Zhengyu Liu, Senior Research Scientist
Karthian R. Jadhav, Graduate Research Assistant
Bridge Engineering Center, Iowa State University

Authors
Zhengyu Liu, Brent M. Phares, and Karthian R. Jadhav

A report from
Bridge Engineering Center
Iowa State University
2711 South Loop Drive, Suite 4700
Ames, IA 50010-8664
Phone: 515-294-8103 / Fax: 515-294-0467
https://intrans.iastate.edu/

TABLE OF CONTENTS

LIST OF FIGURES

LIST OF TABLES

ACKNOWLEDGMENTS

EXECUTIVE SUMMARY

A prior project (Deng and Phares 2016) indicated that the roughness at the entrance to bridges is a primary influence on the general bridge dynamic impact response. The objectives of this project were to correlate international roughness index (IRI) data (which are widely collected and directly related to bridge deck roughness) to impact factors and develop a process for determining the impact factor to use for all bridges in Iowa.To achieve the project objectives, a sample of 20 bridges was selected for bridge monitoring to collect dynamic strain data.

To estimate the static strain data, the locally weighted scatterplot smoothing (LOWESS) function was used to smooth the dynamic strain time history. The dynamic impact factor (DIF) value was then calculated using maximum dynamic and static strain data. IRI data were extracted from PathWeb, a web-based application provided by the Iowa Department of Transportation (DOT) for all bridges considered in the field test program. Once the bridge was identified in PathWeb, the IRI data from four locations near each bridge deck approach were extracted and used to study the relationship between the IRI and DIF. Based on the results from this research, these were the key findings:

- The DIF value decreases as the bridge skew angle increases. Based on linear regression, the DIF value decreases about 0.037 to 0.043 per 10-degree increment of bridge skew.
- The DIF value decreases as the bridge deck condition index increases, meaning that the dynamic response is lower when the bridge deck condition is better.
- For bridges with zero skew, the DIF value increased by 0.006 per 100 in/mile increment of the IRI value.

According to the research findings, an equation was developed for the prediction of DIF on existing bridges with consideration of the bridge skew and the maximum IRI value near the bridge deck approach. Although the proposed equation was validated using data from 13 bridges, the researchers recommend using the equation with the limitation that the actual bridge dynamic response could deviate ±10% from the equation predicted value.

CHAPTER 1. INTRODUCTION

1.1 Background and Problem Statement

A previous project completed by the Iowa State University Bridge Engineering Center, Investigation of the Effect of Speed on Dynamic Impact Factor for Bridges with Different Entrance Conditions (Deng and Phares 2016), determined that the roughness at the entrance to bridges is a primary influence on general bridge dynamic impact factors (DIFs).

With that project, a field test program was conducted on five bridges (two steel girder bridges, two prestressed concrete girder bridges, and one concrete slab bridge) to investigate the dynamic response of bridges due to vehicle loadings. The important factors considered during the field tests included vehicle speed, entrance conditions, vehicle characteristics (i.e., empty dump truck, full dump truck, and semi-truck), and bridge geometric characteristics (i.e., long span and short span).

Three bridge deck entrance conditions were also considered—As-is, Level 1, and Level 2— which simulated different levels of roughness near the bridge deck approach. The field data were then analyzed to derive the DIFs for all gauges installed on each bridge under the different loading scenarios. The project had the following findings:

- The DIF increases with the increase of truck speed, entrance condition roughness level, and bridge span length.
- For all investigated bridges under Level 1 and Level 2 entrance conditions (rough conditions), the DIFs exceeded 1.3; under the As-is entrance conditions (no special surface treatment), the DIFs were less than 1.3 for the steel and concrete girder bridges and less than 0.1 for the concrete slab bridges.
- The empty dump truck induced the greatest impact factors, followed by the full dump truck and the semi-truck.

Based on these findings, the research team concluded that bridges of "normal" roughness likely had DIFs less than codified values. Therefore, the result of using code values may be overly restrictive when considering the issuance of permits. As a result, the researchers recommended that the Iowa Department of Transportation (DOT) consider ways to indirectly determine the impact factor and that the road roughness information (international road index [IRI] data) might be used as an indicator of the entrance condition and, therefore, the impact factor.

Given that bridge deck entrance condition had a substantial impact on the DIF, readily available IRI data could be used as a tool to assign DIFs without the need for time- and resource-intensive testing of all bridges. If successful, the IRI data could then be used to estimate DIF values to use in permitting analysis.

1.2 Objectives

The impetus for this project was to provide information and guidance for eventual use by the Iowa DOT on the allowable speeds for permit vehicles and other heavy loads on bridges. The objectives of this project were to correlate IRI data to impact factors based on the IRI data collected at bridge ends and to develop a process for determining the impact factor to use for every bridge on the state highway system in Iowa in evaluating a bridge's capacity to carry a given vehicle.

1.3 Research Plan

To achieve the project objectives, the following research plan that included close communication with a technical advisory committee (TAC) was undertaken:

Task 1 – Hold Kick-off Meeting with the TAC
Task 2 – Develop Method to Extract IRI Data
Task 3 – Collect DIF Data
Task 4 – Develop Process for Calculating Impact Factors
Task 5 – Review Results for Efficacy
Task 6 – Report

CHAPTER 2. INFORMATION COLLECTION

While a comprehensive literature review was conducted in the first phase of this research (Deng and Phares 2016), a refined review was performed in this phase to elaborate on the terms, concepts, and previous research outcomes that are related to the research topic. The concept of the DIF and the factors that may influence the bridge dynamic response were reviewed and are presented in this section.

Vehicles traveling over bridges induce a dynamic response of the bridge superstructure, which can produce greater live load moments and shears than the static response. The factor used to account for this response is called the dynamic impact factor, abbreviated as IM or DIF. This factor is calculated utilizing equation (1) based on the dynamic as well as static responses (Deng et al. 2014).

$$IM = \frac{R_{dyn} - R_{sta}}{R_{sta}}$$
(1)

where R_{dyn} and R_{sta} are the maximum dynamic and static responses, respectively, regardless of whether the two responses occur with the truck at the same longitudinal position.

The IM is often referred to as the dynamic load allowance (DLA). According to the American Association of State Highway and Transportation Officials (AASHTO) Load and Resistance Factor Design (LRFD) Bridge Design Specifications, the DLA (or IM) is applied to the static design load to account for the dynamic response generated by the moving vehicles. For strength designs of most bridge components (except for deck joints), a DLA of 0.3 should be applied (AASHTO 2010).

In some research, the bridge dynamic impact factor has been abbreviated as DIF and defined as equation (2) (Deng and Phares 2016).

$$DIF = 1 + \frac{R_{dyn} - R_{sta}}{R_{sta}}$$
(2)

To keep consistent with the first phase of this research (Deng and Phares 2016), DIF is used to refer to the bridge live load plus induced dynamic response.

Parameters that influence the bridge DIF have been researched for many years. Cantieni (1983) documented 60 years of Swiss Federal Laboratories for Material Testing and Research (EMPA) experience in the dynamic testing of highway bridges in Switzerland. The goal of the report was to achieve results in dynamic load tests, which are as conclusive as static tests. The work conducted by Cantieni (1983) investigated the impact of dynamic load on short- and long-span bridges, and the results showed a poor correlation between DIF and bridge span length.

Chang and Lee (1994) studied the dynamic behavior of simple-span bridges with rough surfaces under heavy truck loads. Causes of vibration and dynamic behavior of bridges were investigated in both the time and frequency domains. Dynamic responses from four different vehicle models were compared to find an appropriate vehicle model for vibrational analysis. The suggested vehicle model was used to calculate impact factors with different vehicle speeds, deck roughness, and span lengths. The data obtained from the study were used to derive empirical formulas for impact factors represented in terms of span length, vehicle speed, and surface roughness using multiple linear regression. The results showed that DIF does not vary significantly with bridge span length.

Memory et al. (1995) conducted a parametric study using a finite element (FE) model (or FEM) of a continuous beam bridge. The goal was to investigate the effect of support fixity and skew angle on bridge fundamental frequency. Two extreme transverse support conditions—fully fixed and fully released—were considered for bridges with skew angles of 10°, 15°, 20°, and 30°. The fully fixed support represented a post-tensioned concrete deck with strong diaphragm action, while the fully released support represented girder and slab structures. The results of the investigation showed that, in the case of fully released supports, the fundamental frequency remained constant for all skew angles. In the case of fully fixed supports, the fundamental frequency increased with an increase in skew angle, indicating that greater skew angles will have a lower DLA.

Schwarz and Laman (2001) conducted field tests on three prestressed concrete I-girder bridges to obtain the DLA, girder distribution factors (GDFs), and service level stress. Bridge response was measured at each girder with the passage of test trucks and normal traffic. Numerical models (grillage) were then developed for each of the three tested bridges and validated against the field collected data. The results showed a high variation in the DIF values when the bridge span changes. This showed no significant relationship between the DIF and span length.

Li (2005) investigated the dynamic response of bridges due to bridge-vehicle interaction. The evaluation was conducted on multi-girder highway bridges with medium span lengths (50–100 ft) subjected to overweight, oversize vehicles. The effects of various bridge parameters, including road roughness, bridge length, vehicle weight, vehicle speed, and vehicle/bridge frequency ratio, on the bridge response, were investigated. Static and dynamic responses from a selected three-span bridge with simple supported, prestressed concrete girders were collected and analyzed. The FE model was developed based on a field monitored bridge and validated against the field test data. The results indicated no specific relation between the DIF and bridge span length. The research also found that the DIF will be amplified when the resonance of the vehicle-bridge system reaches the fundamental frequency of the bridge.

Deng and Cai (2010) developed a three-dimensional (3D) vehicle-bridge coupled model to simulate the interaction between bridges and vehicles to investigate the impact factor on multi-girder concrete bridges. An HS20-44 truckload was simulated to interact with the deck surface of the FE model. Based on the results, the researchers found that the impact factor was highest at a truck speed of 30 km/h and then dropped as speed increased. This drop in the impact factor was seen from 18.64 mph (30 km/h) to 46.6 mph (75 km/h) and then increased thereafter.

Deng et al. (2014) reviewed and summarized the findings of the studies over the past two decades (from 1994 to 2014) on the parameters that may affect the bridge DIF. These parameters included the span length of the bridge, the fundamental frequency of the bridge, vehicle speed, vehicle weight, vehicle loading position, IRI or road conditions, entrance condition of the bridge, and bridge material. It was found that, in general, DIF is large in the case of lighter vehicles since the corresponding static response is small. While vehicle weight and speed play a significant role in influencing the DIF, vehicle load position also showed some influence on the bridge DIF.

Deng and Phares (2016) collected DIF data when empty dump trucks, full dump trucks, and semi-trucks passed over five different bridges. The following entrance roughness conditions were evaluated: As-is, Level 1, and Level 2. Level 1 was simulated by placing a ramp at a distance of 10 ft from the bridge deck approach joint. Level 2 was simulated by placing the ramp directly over the joint. The results indicated that the DIF increases with the increase of surface roughness, the DIFs increase as the static strain decreases, and the DIFs are sensitive to low strains. Accordingly, the DIFs related to the greater strains were deemed more reliable. The researchers found that, in the case of steel girders and prestressed concrete girder bridges, the DIF for long bridges was lower than that for short bridges. Results also showed that, in all bridges, the DIF was high for vehicles at high speed. The DIF ranged from 1 to 1.1 at crawl speed and 1.3 to 2 at 50 mph.

Mohseni et al. (2018) presented a method for determining DIFs for skewed, composite, slab-on-girder bridges under AASHTO LRFD truck loading. An extensive parametric study of 125 bridges with different key parameters, including skew angle, was conducted. The research showed that the effect of skew angle on impact factor was low (<10%) for angles less than 45° and did not vary too much, but drastically increased on bridges with a skew angle more than 45°.

Although many efforts have been put toward determining the factor that dominates the bridge DIF, not all studies show agreement. For example, several studies (Cantieni 1983, Billing and Green 1984, Memory et al. 1995) proposed empirical formulas to state the relationship between bridge fundamental frequency and span length. These formulas vary in mathematical form but, in general, imply that large span lengths have a low fundamental frequency. This increases the possibility of the vehicle frequency reaching the natural frequency of the bridge with a long span at a lower dynamic response than for a short span, therefore increasing the DIF. However, the literature review results from Deng and Phares (2016) and Deng et al. (2014) indicated that the relationship between DIF and span length is unclear.

Based on the information collected, researchers found that bridge skew has a consistent result on the effects of the DIF and that the DIF decreases as bridge skew increases (Mohseni et al. 2018, Memory et al. 1995). With respect to the bridge condition, researchers found that the DIF increases with the deck surface roughness at the bridge approach.

CHAPTER 3. DIF DATA GENERATING AND ANALYSIS

This chapter documents the procedures followed to generate the DIFs for several bridges in Iowa. To measure the bridge dynamic response subject to the live load, a sample of bridges was identified and instrumented with strain gauges. The dynamic field-measured strain data from ambient traffic were then smoothed using the locally weighted scatterplot smoothing (LOWESS) function to estimate the static strain response. The maximum measured dynamic strain and estimated static strain were used to calculate the DIF for each truck event and each bridge.

3.1 Bridge Selection

The entire Iowa DOT state-owned bridge population was considered, and sample bridges were selected that closely matched the distribution of bridge attributes across the state. Bridge attributes deemed important for distribution matching included length, skew angle, age, material, and structure type. Other considerations for bridge selection were National Bridge Inventory (NBI) average daily traffic (ADT) and NBI average daily truck traffic (ADTT) to ensure that bridges had adequate traffic when collecting data.

Initially, a sample of 40 bridges in Iowa was identified. Table 1 lists the 40 bridge candidates with bridge information, including bridge ID, year built, skew angle, superstructure material, structure type, bridge total length, span length, average daily traffic, average daily truck traffic percent, and average daily truck traffic volume.

The bridges selected were state-maintained bridges. Note that, during the initial selection process, bridges with less than 5% truck traffic and less than 2,000 ADT were eliminated from further consideration. Additionally, site accessibility (e.g., need for traffic control and distance from Ames, Iowa) was initially considered.

Table 1. Preliminary selection – 40 bridges for field test

No	Bridge ID	Year Built	Skew Angle	Superstructure Material	Structure Type	Total Length (ft)	Span Length (ft)	ADT	ADDT Percent	ADDT Volume
1	0737.8S057	2010	0	Concrete continuous	Slab	133	39.5	2,640	5	132
2	0831.6R030	1963	0	Steel continuous	Girder and Floor-beam	724	85.25	4,500	12	540
3	2510.3S006	2015	0	Prestressed concrete	Multi-beam or Girder	389	91	6,200	8	496
4	2518.0R080	1966	15	Steel continuous	Multi-beam or Girder	204	61	21,250	20	4250
5	2528.6R141	1976	9	Concrete continuous	Slab	111	33.8	2,270	11	249.7
6	3836.7S057	1986	15	Concrete continuous	Slab	113	33.5	2,640	5	132
7	4045.2R035	1972	7	Prestressed concrete	Multi-beam or Girder	265	68.25	8,250	27	2,227.5
8	4045.4R020	1975	0	Prestressed concrete	Multi-beam or Girder	138	39.1	5,050	23	1,161.5
9	4048.9R035	1972	30	Concrete continuous	Slab	93	27.5	8,000	28	2,240
10	4050.0S017	1974	4	Prestressed concrete	Multi-beam or Girder	268	40.75	6,700	7	469
11	4263.4L020	1999	0	Prestressed concrete	Multi-beam or Girder	171	51.5	4,450	27	1,201.5
12	5007.7S117	1967	0	Steel continuous	Multi-beam or Girder	322	70	5,400	8	432
13	5076.6R080	1962	0	Prestressed concrete	Multi-beam or Girder	183	55.5	15,400	25	3,850
14	6485.3L030	1995	0	Steel continuous	Multi-beam or Girder	272	71.75	2,850	27	769.5
15	7700.2O235	1966	8	Steel continuous	Multi-beam or Girder	222	46	15,200	23	3,496
16	7704.1R235	1967	5	Concrete continuous	Slab	231	42.5	55,100	5	2,755
17	7707.5R235	2006	30	Steel continuous	Multi-beam or Girder	315	80	44,950	7	3,146.5
18	7708.5S235	1962	18	Steel continuous	Multi-beam or Girder	864	45	93,500	6	5,610
19	7727.5R080	1958	11	Prestressed concrete	Multi-beam or Girder	252	55.5	36,650	19	6,963.5
20	7730.5L080	1958	0	Prestressed concrete	Multi-beam or Girder	127	39	48,450	17	8,236.5

Table 1. Preliminary selection – 40 bridges for field test (continued)

No	Bridge ID	Year Built	Skew Angle	Superstructure Material	Structure Type	Total Length (ft)	Span Length (ft)	ADT	ADDT Percent	ADDT Volume
21	7734.7L080	1958	0	Prestressed concrete	Multi-beam or Girder	112	34.75	50,250	16	8,040
22	7768.5L035	2003	0	Steel continuous	Multi-beam or Girder	656	105	27,750	13	3,607.5
23	7769.0R035	2014	13	Prestressed concrete	Multi-beam or Girder	197.1	41	24,700	13	3,211
24	7771.5R035	2014	10	Prestressed concrete	Multi-beam or Girder	447.1	86	39,150	10	3,915
25	7774.0L065	1997	3	Steel continuous	Multi-beam or Girder	297	76	10,650	12	1,278
26	7774.0R065	1997	3	Steel continuous	Multi-beam or Girder	299	76	10,650	12	1,278
27	7780.8L065	1994	17	Prestressed concrete	Multi-beam or Girder	201	55.75	14,650	14	2,051
28	7788.3L035	2002	45	Prestressed concrete	Multi-beam or Girder	282	105.75	45,300	11	4,983
29	7793.6L035	2018	15	Prestressed concrete	Multi-beam or Girder	197.1	61	26,200	16	4,192
30	7926.5S146	2005	30	Prestressed concrete	Multi-beam or Girder	171	43.25	2,200	6	132
31	7984.7L080	1963	0	Concrete continuous	Slab	114	34.25	14,500	26	3,770
32	8601.1L030	2010	0	Prestressed concrete	Multi-beam or Girder	158.5	55.75	9,200	13	1,196
33	8603.3R030	2009	29	Prestressed concrete	Multi-beam or Girder	212.4	46	3,300	16	528
34	9106.6S028	1983	0	Prestressed concrete	Multi-beam or Girder	238	76.5	6,000	9	540
35	9167.8L065	2013	0	Prestressed concrete	Multi-beam or Girder	349	86	10,050	5	502.5
36	9167.8R065	1970	5	Steel continuous	Multi-beam or Girder	325	97.5	10,100	5	505
37	9179.1L005	1997	0	Prestressed concrete	Multi-beam or Girder	306	96	4,400	8	352
38	9466.0S007	1974	0	Concrete continuous	Slab	133	39.5	2,590	12	310.8
39	9962.1S069	1928	0	Steel	Multi-beam or Girder	33	32	2,280	16	364.8
40	9965.3S017	1933	0	Steel continuous	Multi-beam or Girder	213	64	3,210	17	545.7

To verify that the selected 40 bridges were representative of the Iowa bridge population, Table 2 was created to compare the attributes of the Iowa bridge population and the selected 40 bridges.

Table 2. Iowa population vs. bridge selection

Bridge parameters	Iowa population	Preliminary selection – 40 bridges
Avg. Year Built	1981	1983
Avg. Length	260 ft	258 ft
Avg. Skew Angle	13°	8°
Material	56% Prestressed Concrete	50% Prestressed Concrete
Structure Type	80% Multi-beam or Girder	80% Multi-beam or Girder

The bridge parameters used for the evaluation included year built, bridge length, skew angle, superstructure material, and structure type. These bridge parameters were selected because the literature indicated they might be related to the bridge dynamic response and to ensure broader applicability of the research results. The data in Table 2 indicated that the selected bridges have similar average characteristics to that of the state bridge population.

To further validate the selected samples, the distribution of each bridge attribute, including year built, bridge length, skew angle, superstructure material, and structure type, were visually/qualitatively compared for the Iowa population and the sample. Figure 1 through Figure 5 show the comparison results for year built, bridge length, skew angle, superstructure material, and structure type, respectively.

(a) Iowa population   (b) Preliminary selection – 40 bridges
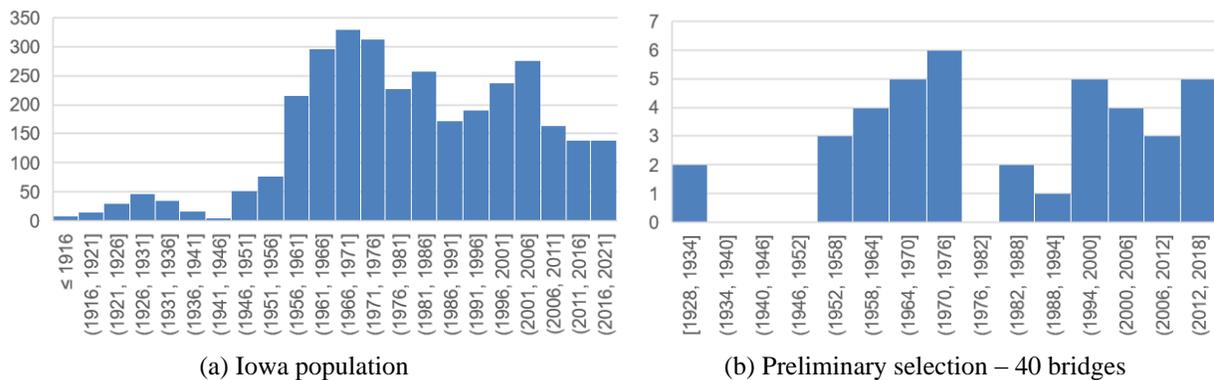
Figure 1. Years built for the bridges

11
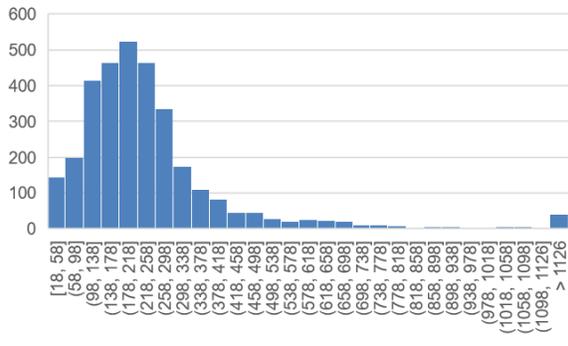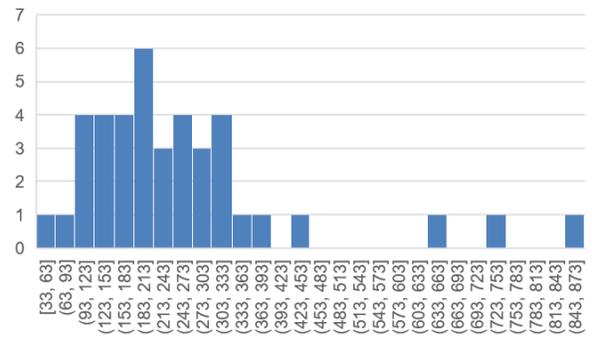
(a) Iowa population　　　　　　　　(b) Preliminary selection – 40 bridges

Figure 2. Bridge lengths
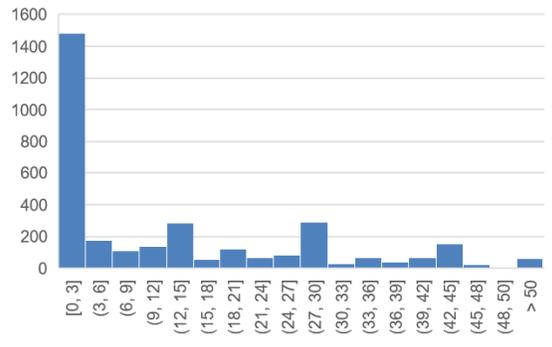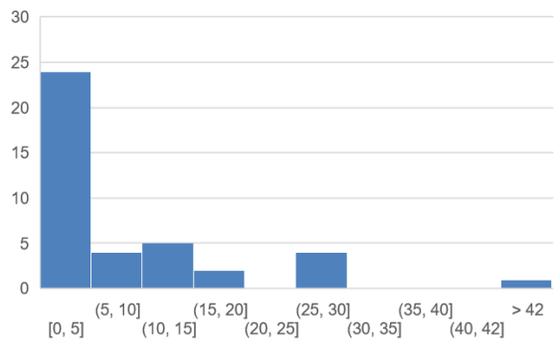
(a) Iowa population　　　　　　　　(b) Preliminary selection – 40 bridges

Figure 3. Bridge skew angles
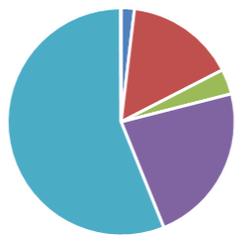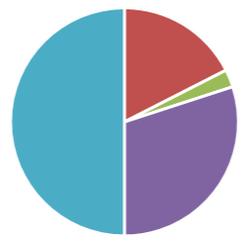
(a) Iowa population　　　　　　　　(b) Preliminary selection – 40 bridges

Figure 4. Bridge girder materials

| (a) Iowa population | (b) Preliminary selection – 40 bridges |
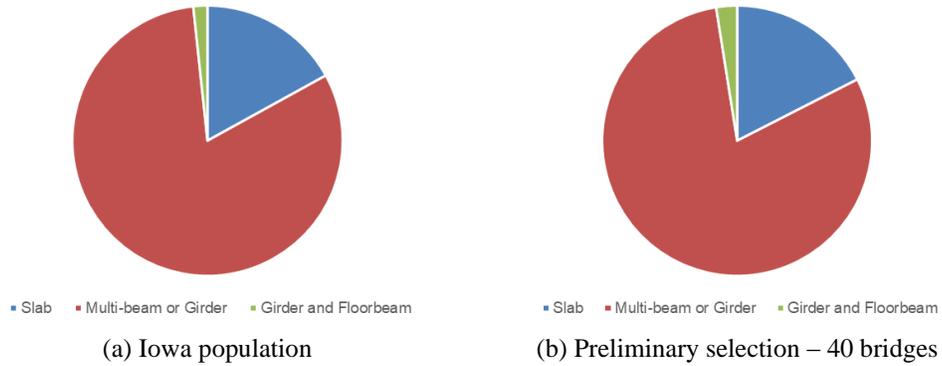
Figure 5. Bridge structure types

The results indicated that the selected bridge samples showed a very close distribution character to that of the Iowa bridge population for each bridge parameter (year built, bridge length, skew angle, superstructure material, and structure type). This indicated that the 40 selected bridges were a good representation of the Iowa bridge population.

To further focus the project effort, the number of bridges to be utilized in the field test program was reduced to 20. The bridges were narrowed down by location, ease of access, and Iowa DOT cross-referencing of bridges that recently had construction or renovations since the IRI values were collected. The final 20 bridges with relevant bridge parameters are tabulated in Table 3.

Table 3. Final bridge list for field testing

No.	Bridge ID	ADT	ADTT	Material	Structure	Skew Angle	Length (ft)	Deck Condition*	Span Length (ft)
1	0831.6R030	4,000	520	Steel continuous	Girder and Floor-beam	0	659	6	85.25
2	4045.2R035	7,050	2,256	Prestressed concrete	Stringer/Multi-beam	7	265	7	68.25
3	4045.4R020	4,500	1,125	Prestressed concrete	Stringer/Multi-beam	0	138	6	39.1
4	4263.4L020	3,950	1,185	Prestressed concrete	Stringer/Multi-beam	0	171	7	51.5
5	5007.7S117	4,810	433	Steel continuous	Stringer/Multi-beam	0	322	7	70
6	5076.6R080	13,100	3,930	Prestressed concrete	Stringer/Multi-beam	0	183	6	55.5
7	6485.3L030	2,500	775	Steel continuous	Stringer/Multi-beam	0	272	8	71.75
8	7707.5R235	45,000	3,150	Steel continuous	Stringer/Multi-beam	30	155.8	7	80
9	7708.5S235	78,300	5,481	Steel continuous	Stringer/Multi-beam	18	864	7	45
10	7730.5L080	40,550	8,110	Prestressed concrete	Stringer/Multi-beam	0	125	5	39
11	7769.0R035	20,650	3,304	Prestressed concrete	Stringer/Multi-beam	13	197.1	8	41
12	7774.0R065	9,500	1,235	Steel continuous	Stringer/Multi-beam	3	299	6	76
13	7780.8L065	12,950	1,943	Prestressed concrete	Stringer/Multi-beam	17	201	7	55.75
14	7788.3L035	37,900	5,306	Prestressed concrete	Stringer/Multi-beam	45	282	6	105.75
15	7793.6L035*	21,950	NA	Prestressed concrete	Stringer/Multi-beam	15	268	7	61
16	7926.5S146	1,960	137.2	Prestressed concrete	Stringer/Multi-beam	30	171	8	43.25
17	7984.7L080	12,350	3,828.5	Concrete continuous	Slab	0	114	5	34.25
18	8601.1L030	8,100	1,215	Prestressed concrete	Stringer/Multi-beam	0	158.5	9	55.75
19	8603.3R030	2,900	551	Prestressed concrete	Stringer/Multi-beam	29	212.4	8	46
20	9167.8L065	8,900	445	Prestressed concrete	Stringer/Multi-beam	0	349	8	86

*Based on NBI data (2022) with values from 1 to 9, with 5 to 9 here indicating FAIR CONDITION to EXCELLENT CONDITION

3.2 Instrumentation Plan

The general instrumentation layout used during each of the bridge tests was developed to capture the dynamic response of the subject bridge to ambient live loads (i.e., traffic loads) to provide the data needed for the calculation of the DIF. To do that, strain gauges were utilized and mounted on the bottom flange of the bridge girders at or near mid-span. These locations usually give "large" strain data values when the bridge is subjected to traffic loads.

Bridge Diagnostic, Inc. (BDI) strain gauges were used to instrument each bridge and were recorded at a rate of 1,000 data points per second. For multi-span bridges, the gauges were placed in the first span near the bridge deck approach. Figure 6 shows a typical instrumentation plan for a steel girder bridge.
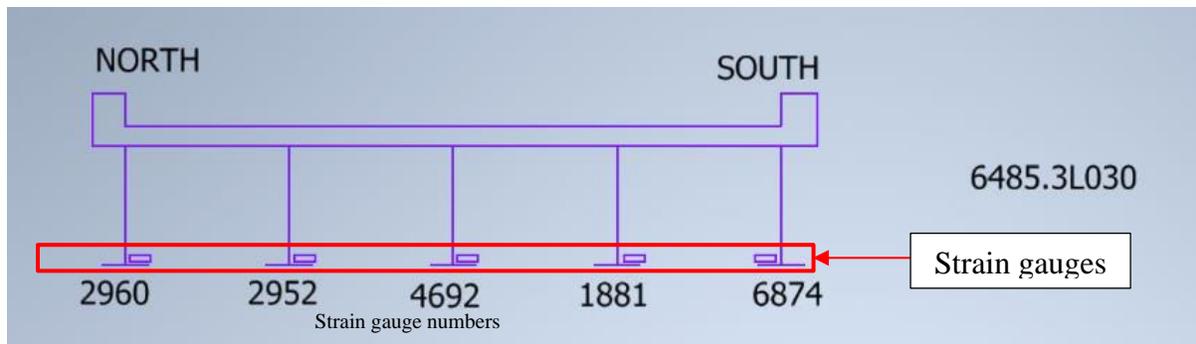
Figure 6. Instrumentation plan for Bridge 6485.3L030

Each girder was instrumented with a strain gauge, which was always mounted on the bottom flange. Figure 7 shows images of typical field-mounted strain gauges.

| (a) Concrete girders | (b) Steel girders | (c) Steel girders |

Figure 7. Strain gauge mounting techniques

For concrete girders, the gauges were mounted on the outside edge of the flange (Figure 7a), and, for steel girders, gauges were mounted on either the bottom or top of the bottom flange, depending on accessibility (Figure 7b and 7c). One slab bridge was included in the field test program, and five strain gauges were mounted to the underside of the slab with equal spacing and installed with gauge extenders.

In addition to the dynamic strain data, videos of traffic passing over the bridge were recorded during the field monitoring to provide documentation of the truck event.

3.3 Field Data Interpretation

Each bridge was monitored for a minimum of 10 minutes to collect data for a number of different truck types. Videos of the field testing were captured to identify the times, lanes, and types of trucks passing over the bridge.

Given that the intent of the project was to provide guidance on the DIF for heavy vehicles, truck traffic was the primary interest of this study. When the data were analyzed, trucks were categorized into five possible categories: 3-axle trucks, fully/partially loaded 5-axle tractor/trailers, empty 5-axle tractor/trailers, 6-axle or more tractor/trailers, and other trucks. Examples of each of these categories are shown in Figure 8.

Empty 5-axle

Fully/Partially Loaded 5-axle

6+ axle

Other-1

Other-2

Figure 8. Truck categories

In most cases, data were collected when no other vehicles were on the bridge to isolate the effect of a single truck. Some longer bridges with higher traffic volumes had data points with passenger vehicles remaining on the bridge when the truck entered the first span. This most likely dampened the effect of the DIF but was only the case in a small percentage of data points and was believed to have minimal effect on the dynamic response.

For this work, the trucks were estimated to be either empty or non-empty based on visual observation for flatbed trailers, the difference in strain between the tractor axles and trailer axles, maximum strain values across multiple trucks on the bridge, or a combination of these methods. Such differentiation helped to focus the data analysis on different classes of vehicles.

3.4 Determination of Bridge Static Response (LOWESS Function)

The data collected from the field monitoring captured the bridge dynamic response resulting from the traffic load. To calculate the DIF, bridge static response subject to the same traffic load is needed. However, unlike the research conducted by Deng and Phares (2016), the static strain was not possible to measure through crawl speed because ambient traffic was utilized for the live loading.

Instead, the method used in this analysis was to fit a curve to the dynamic strain data to estimate the static response. To estimate the bridge static strain, the LOWESS function was used to find the static strain response from the dynamic response data.

The LOWESS function is a local polynomial regression method used to fit a smooth curve between two variables (Cleveland 1979). For scatterplots of points (x_i, y_i), for i=1, 2, ..., n, summarized by another set of points $(x_i, \hat{y}_i)$, for i=1, 2, ..., n, where the initial fitted value $\hat{y}_i$ at each x_i, is the fitted value of dth degree polynomial fit to the data using weighted least squares with weights $w_k(x_i)$. Weights can be calculated using equation (3).

$$w_k(x_i) = W\left(\frac{x_k - x_i}{h_i}\right) \text{ for i, k} = 1, ..., n \tag{3}$$

where h_i is the distance from x_i to the rth nearest neighbor of x_i, and W is the weight function with the following properties:

- W(x) > 0 for |x| < 1
- W(-x) = W(x)
- W(x) is a nonincreasing function for x ≥ 0
- W(x) = 0 for |x| ≥ 1

Estimates of parameters $\hat{\beta}_{j.}(x_i)$, $j = 0, 1, ..., d$, where d is the degree of the polynomial, are computed for the polynomial regression of y_k on x_k, which is fitted by weighted least squares with weight $w_k(x_i)$ for data (x_k, y_k). $\hat{\beta}_j(x_i)$ are the values of β_j that minimize the function given in equation (4):

$$\sum_{k=1}^{n} w_k(x_i)\left(y_k - \beta_0 - \beta_1 \times x_k - \cdots - \beta_d \times x_k^d\right)^2 \tag{4}$$

The point $x_i, \hat{y}_i$ is the smoothed point at x_i found using locally weighted regression of degree d, where the fitted value, $\hat{y}_i$, of regression at x_i is given by equation (5).

$$\hat{y_i} = \sum_{j=0}^{d} \widehat{\beta}_J \times x_i \times x_i^j, \text{ for j=1, ..., n} \tag{5}$$

The smoother span of the function, known as the f-value, represents the proportion of data neighboring the x_i that were used for the smoothing. A smaller f-value selects an insufficient amount of data around x_i, resulting in a large variance. Larger than the required f-value makes the regression over-smooth, which results in a loss of data. Therefore, it becomes necessary to choose a reasonable f-value to minimize the variability in the smoothed points without distorting the data, as stated by Cleveland (1979).

To better estimate which f-value was appropriate to use to reduce error, other areas of the data where no vehicle was on the bridge were analyzed to determine the best fit. The f-value that can create the static response close to zero when no vehicle was on the bridge was used as the best fit.

3.5 Strain Data and DIF Calculation

Once the static response was determined, the maximum dynamic strain and maximum static strain were extracted from each truck event and used to calculate the DIF utilizing equation (6).

$$DIF = 1 + \frac{\varepsilon_d - \varepsilon_s}{\varepsilon_s} \tag{6}$$

where ε_d is the maximum dynamic strain obtained from the strain gauges, and ε_s is the maximum static strain found by curve-fitting the dynamic strain time history.

As an example, images of several trucks that produced a significant response on Bridge 6485.3L030 are shown in Figure 9 through Figure 14.

Truck event 1

Max Dynamic Strain: 42   Max Static Strain: 32   DIF: 1.29   Truck weight: Empty   Lane: Right
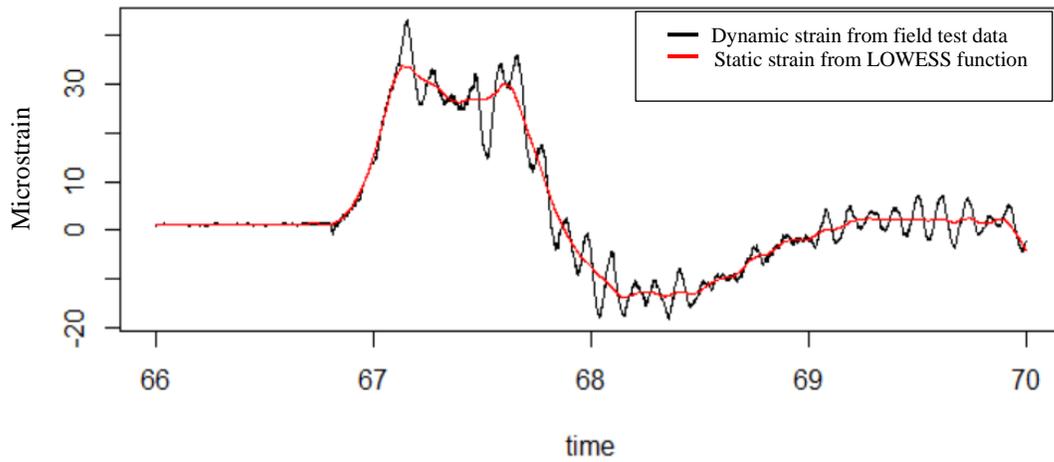
Strain time history of Truck event 1

Figure 9. Data of Truck event 1 on Bridge 6485.3L030

Truck event 2

Max Dynamic Strain: 51   Max Static Strain: 49   DIF: 1.03   Truck weight: Empty   Lane: Right
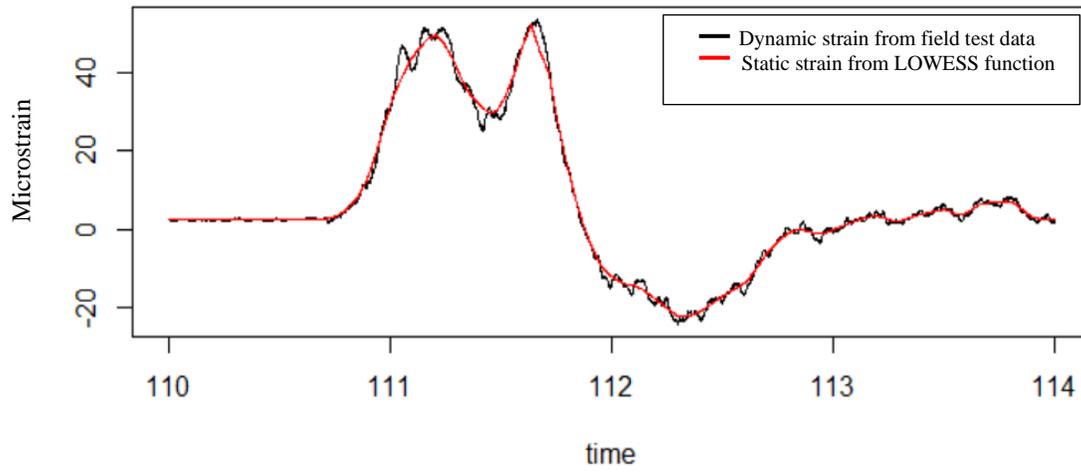
Strain time history of Truck event 2

Figure 10. Data of Truck event 2 on Bridge 6485.3L030

Truck event 3

Max Dynamic Strain: 94   Max Static Strain: 94   DIF: 1.04   Truck weight: Non-Empty   Lane: Right
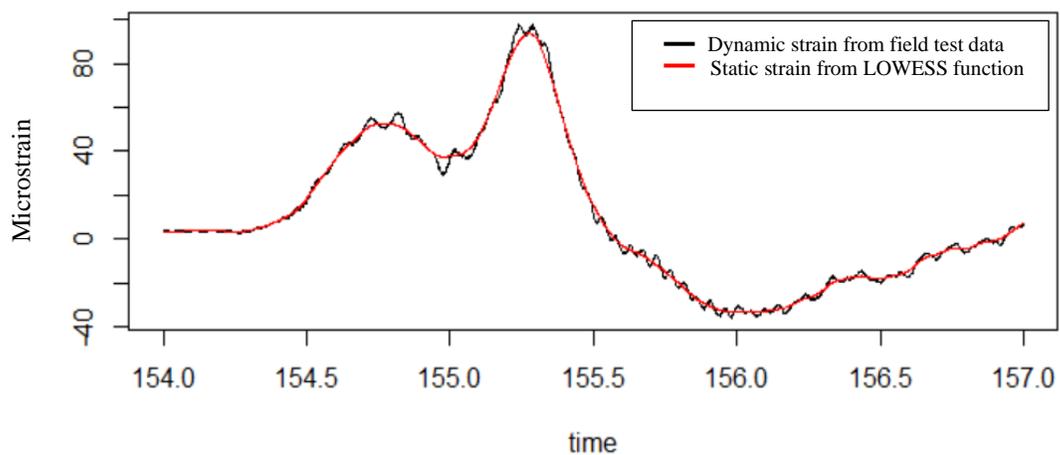
Strain time history of Truck event 3

Figure 11. Data of Truck event 2 on Bridge 6485.3L030

22

Truck event 4

Max Dynamic Strain: 35   Max Static Strain: 25   DIF: 1.43   Truck weight: Empty   Lane: Left
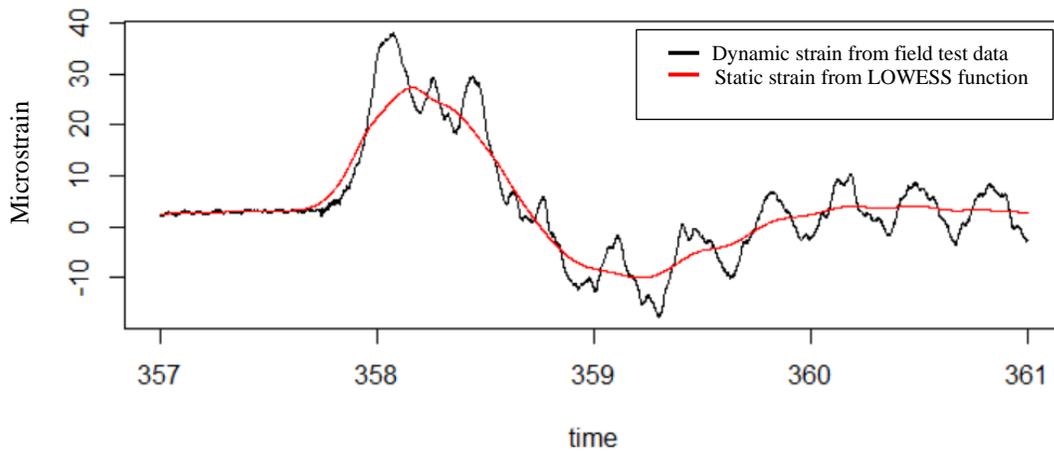
Strain time history of Truck event 4

Figure 12. Data of Truck event 4 on Bridge 6485.3L030

Truck event 5

Max Dynamic Strain: 90 Max Static Strain: 78 DIF: 1.15 Truck weight: Non-Empty Lane: Right
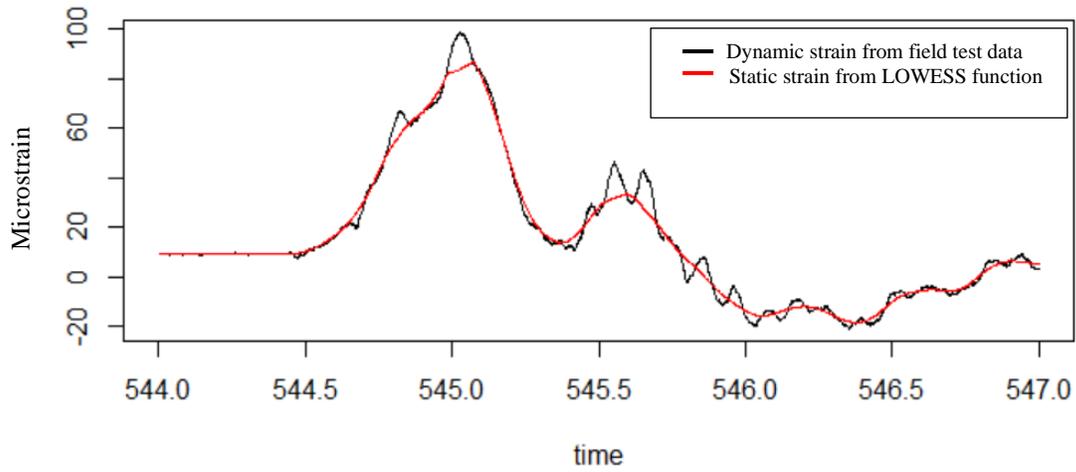

Strain time history of Truck event 5

Figure 13. Data of Truck event 5 on Bridge 6485.3L030

Truck event 5

Max Dynamic Strain: 82   Max Static Strain: 72   DIF: 1.13   Truck weight: Non-Empty   Lane: Right
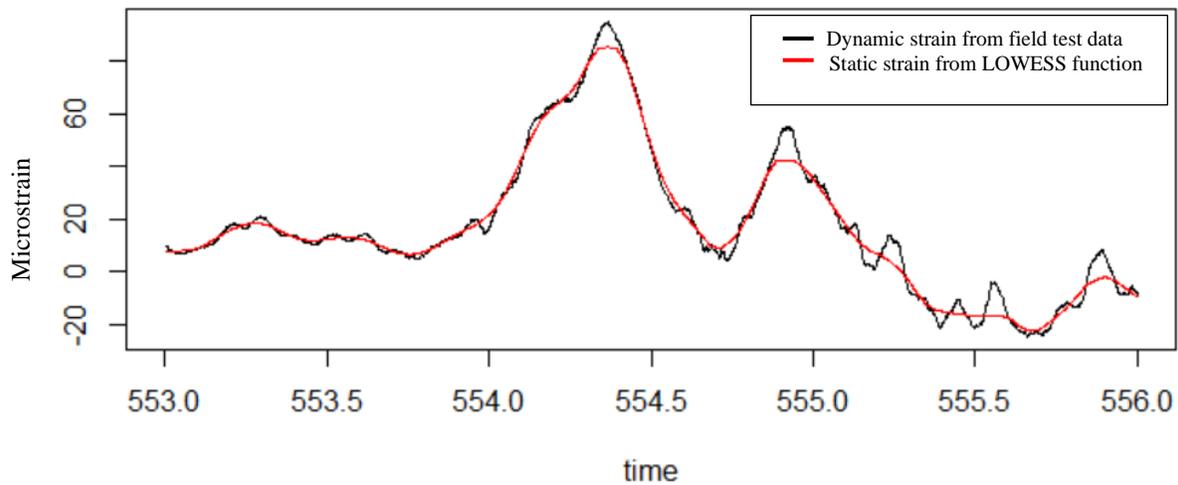
Strain time history of Truck event 6

Figure 14. Data of Truck event 6 on Bridge 6485.3L030

Using each truck event, the maximum dynamic and static strain were used to calculate the DIF for the bridge.

The same procedure was applied to the data collected from all 20 bridges tested. Table 4 shows the tabulation of the DIF, the lane location, estimated truck weight, and vehicle speed for each truck event (labeled Vehicle 1–6 in the column headings).

Table 4. Calculated DIF for 20 tested bridges

Bridge ID.		Vehicle 1	Vehicle 2	Vehicle 3	Vehicle 4	Vehicle 5	Vehicle 6
4045.2R035	DIF	1.138	1.194	1.149	1.101	1.156	
	Lane	Right	Right	Right	Right	Right	
	Load	Non-Empty	Non-Empty	Non-Empty	Empty	Empty	
	Estimated vehicle speed (mph)	65	65	65	65	65	
0831.6R030	DIF	1.167	1.113	1.113			
	Lane	Right	Right	Right			
	Load	Empty	Empty	Non-Empty			
	Estimated vehicle speed (mph)	70	70	65			
7984.7L080	DIF	1.358	1.054	1.030	1.113	1.252	
	Lane	Right	Right	Right	Right	Right	
	Load	Empty	Empty	Empty	Empty	Empty	
	Estimated vehicle speed (mph)	70	70	70	70	70	
7769.0R035	DIF	1.045	1.055	1.042	1.143	1.024	
	Lane	Center	Center	Center	Center	Center	
	Load		Empty	Non-Empty	Empty	Empty	
	Estimated vehicle speed (mph)	65	65	65	65	65	
6485.3L030	DIF	1.288	1.028	1.040	1.427	1.151	1.132
	Lane	Right	Right	Right	Left	Right	Right
	Load	Empty	Empty	Non-Empty	Empty	Non-Empty	Non-Empty
	Estimated vehicle speed (mph)	65	65	65	65	65	65
5007.7S117	DIF	1.255	1.100	1.08			
	Lane	Right	Right	Right			
	Load	Empty	Empty	Empty			
	Estimated vehicle speed (mph)	35	35	35			
7708.5S235	DIF	1.051	1.139	1.081	1.138	1.070	
	Lane	Left	Center Left	Center Left	Center Right	Left	
	Load	Empty	Non-Empty	Non-Empty	Non-Empty	Non-Empty	
	Estimated vehicle speed (mph)	65	65	65	65	65	
7780.8L065	DIF	1.070	1.036	1.050	1.086	1.136	1.007
	Lane	Right	Right	Right	Right	Right	Right
	Load	Non-Empty	Non-Empty	Empty	Empty	Empty	Non-Empty
	Estimated vehicle speed (mph)						
7788.3L035	DIF	1.022	1.010	1.004	1.0138	1.051	1.082
	Lane	Right	Center	Right	Right	Center	Right
	Load	Non-Empty	Non-Empty	Non-Empty	Non-Empty	Non-Empty	Non-Empty
	Estimated vehicle speed (mph)	65	65	65	65	65	65
9167.8L065	DIF	1.044	1.022	1.037	1.052	1.069	
	Lane	Right	Right	Right	Left	Right	
	Load	Non-Empty	Non-Empty	Empty	Empty	Empty	
	Estimated vehicle speed (mph)	60	60	60	60	60	

Table 4. Calculated DIF for 20 tested bridges (continued)

Bridge ID		Vehicle 1	Vehicle 2	Vehicle 3	Vehicle 4	Vehicle 5	Vehicle 6
4045.4R020	DIF	1.264	1.050	1.172	1.127	1.265	
	Lane	Center	Center	Center	Center	Center	
	Load	Empty	Non-Empty	Non-Empty	Non-Empty	Empty	
	Estimated vehicle speed (mph)	65	65	65	65	65	
4263.4L020	DIF	1.099	1.066	1.168	1.232	1.049	
	Lane	Right	Right	Left	Right	Right	
	Load	Empty	Non-Empty	Empty	Empty	Non-Empty	
	Estimated vehicle speed (mph)	65	65	65	65	65	
5076.6R080	DIF	1.472	1.056	1.315	1.137	1.182	
	Lane	Left	Right	Right	Right	Right	
	Load	Empty	Non-Empty	Non-Empty	Non-Empty	Non-Empty	
	Estimated vehicle speed (mph)	65	65	65	65	65	
7707.5R235	DIF	1.0899	1.038	1.031	1.023	1.140	
	Lane	Center	Right	Left	Center	Center	
	Load			Non-Empty		Empty	
	Estimated vehicle speed (mph)	60	60	60	60	60	
7730.5L080	DIF	1.173	1.173	1.526	1.550	1.365	
	Lane	Right	Center	Left	Right	Right	
	Load	Empty	Non-Empty	Empty	Empty	Empty	
	Estimated vehicle speed (mph)	65	65	65	65	65	
7774.0R065	DIF	1.029	1.107	1.051			
	Lane	Center	Center	Left			
	Load	Non-Empty	Empty	Non-Empty			
	Estimated vehicle speed (mph)	65	65	65			
7926.5S146	DIF	1.021	1.008				
	Lane	Right	Right				
	Load						
	Estimated vehicle speed (mph)	55	55				
8601.1L030	DIF	1.165	1.035	1.032	1.026	1.075	
	Lane	Right	Right	Right	Right	Right	
	Load	Empty	Empty	Non-Empty	Non-Empty	Non-Empty	
	Estimated vehicle speed (mph)	65	65	65	65	65	
8603.3R030	DIF	1.058	1.104	1.021	1.046	1.028	
	Lane	Right	Right	Right	Right	Right	
	Load	Empty	Empty	Non-Empty	Non-Empty	Non-Empty	
	Estimated vehicle speed (mph)	65	65	65	65	65	

Note that six truck events were not captured for all bridges. On some bridges, only two to five truck events were captured. The data in Table 4 were used in the subsequent work to study the relationship between the DIF and other parameters, including the IRI.

3.6 Effect of Bridge Parameters

Based on information in the published literature and the first phase of this work (Deng and Phares 2016), the researchers anticipated one or more bridge features might be related to the bridge DIF. These parameters included bridge skew, span length, and bridge deck condition. In this section, the calculated DIF data were plotted against these bridge parameters to investigate the influence of the parameters on the bridge DIF.

Figure 15 plots the DIF values for all 20 bridges tested versus bridge skew.

(a) Average DIF vs. bridge skew   (b) DIF vs. bridge skew
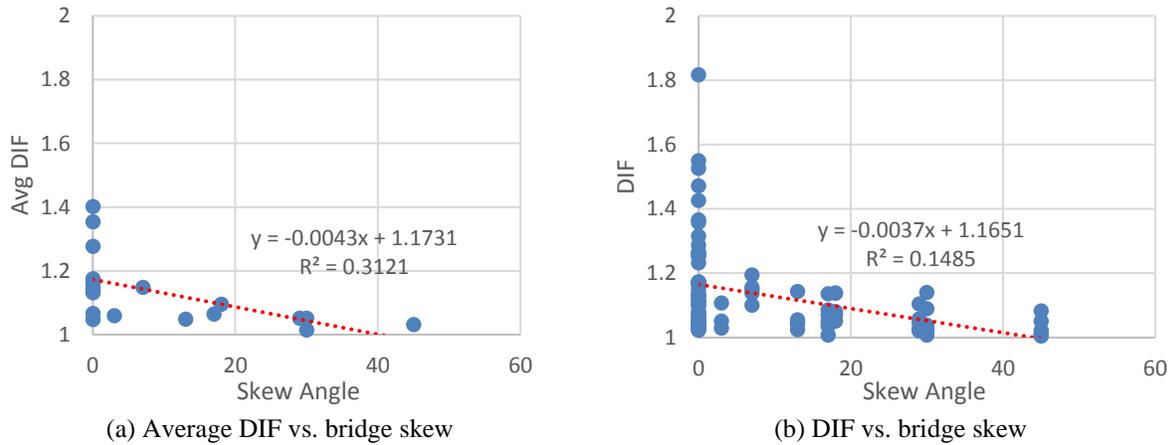
Figure 15. DIF vs. skew angle

During the field monitoring, multiple truck events were captured from each bridge, which resulted in multiple DIF values for a bridge. To present the DIF value for each individual truck event as well as the average DIF for a bridge, two plots were created for each bridge parameter.

Figure 15a shows the average DIF resulting from all the truck events on a bridge versus the skew of that bridge, while Figure 15b plots the DIF value for each truck event versus the skew of the corresponding bridge. On both plots, a linear regression line was created to reflect the data trend.

The R-squared value was generated, which indicates the degree of correlation between the spread data and the regression line. An R-squared value close to 1.0 indicates a good correlation, and a low R-squared value close to 0.0 indicates a poor correlation.

Both plots in Figure 15 indicate that the DIF value decreases as the bridge skew increases. Based on the regression line in the plots, the DIF decreases about 0.037 to 0.043 per 10° increment of bridge skew. This shows agreement with the findings from Memory et al. (1995), which concluded that greater skew angles resulted in a lower DLA.

Figure 16 and Figure 17 were created using the same approach as that used for Figure 15, showing the DIF value versus the bridge deck condition and the DIF value versus the length of the instrumented span, respectively.


(a) Average DIF vs. deck condition   (b) DIF vs. deck condition
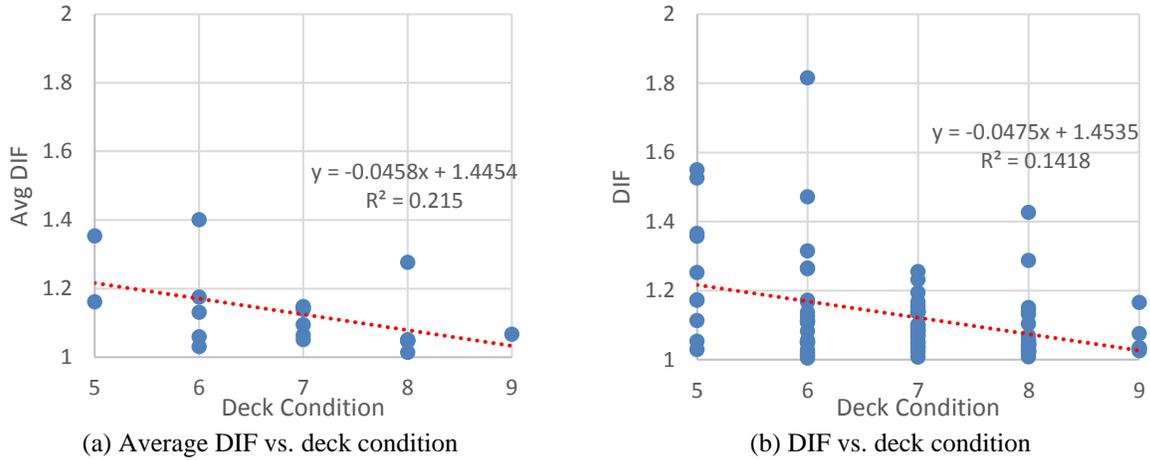
Figure 16. DIF vs. deck condition

(a) Average DIF vs. length of instrumented span   (b) DIF vs. length of instrumented span
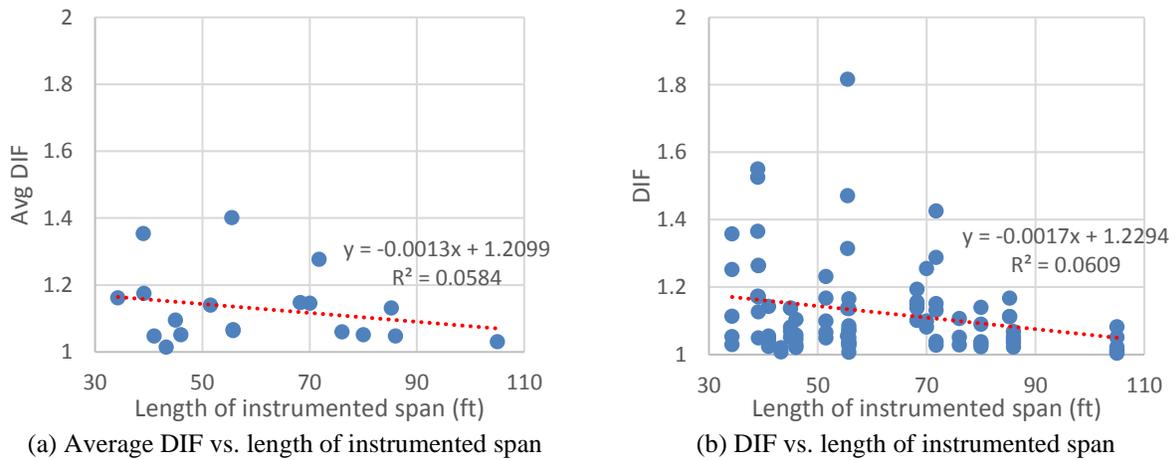
Figure 17. DIF vs. length of instrumented span

NBI data (2022) were used in Figure 16 (and in the previous Table 3) for the deck condition. The NBI data rates the bridge deck condition using values from 1 to 9, with 1 indicating FAILURE CONDITION and 9 indicating EXCELLENT CONDITION. The deck condition of the 20 monitored bridges fell into a range of 5 to 9 or from FAIR CONDITION to EXCELLENT CONDITION.

Both plots in Figure 16 show a consistent trend indicating that the DIF value decreases as the deck condition improves. The regression line for both plots in Figure 17 indicate that the DIF value decreases as the length of the instrumented span increases. However, the low R-squared values (0.0584 and 0.0609) in both plots mean that the correlation between the data and the

regression line is low. Therefore, the researchers concluded that the data in this research were not sufficient to establish the relation between the bridge span length and the DIF value.

CHAPTER 4. IRI DATA EXTRACTION AND ANALYSIS

In collaboration with the Iowa DOT, IRI data were extracted from PathWeb (2022) to allow for the study of any relationships between the IRI data and bridge dynamic behavior. More specifically, the IRI data were downloaded from PathWeb at multiple locations of each bridge and used to seek their relationship to the bridge DIF values estimated in Chapter 3.

4.1 IRI Data Source – PathWeb

PathWeb is a web-based application designed to store road network data. The bridge location information was first identified from the Iowa DOT Structure Inventory and Inspection Management System (SIIMS 2021). Then, this information was input into PathWeb to identify the bridge. Figure 18 shows the input window in PathWeb for the identification of the bridge.
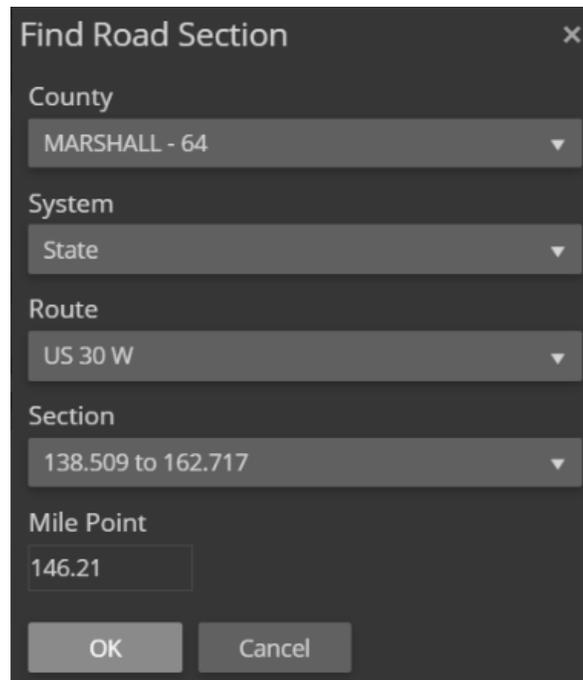
Figure 18. Input window in PathWeb for bridge identification

Figure 19 shows the bridge selected on a map in PathWeb.
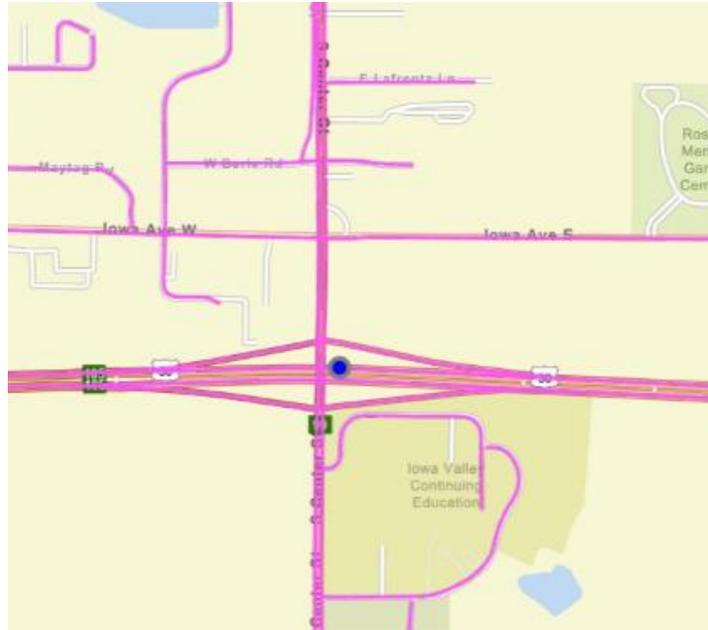
Figure 19. Location of bridge 6485.3L030 on PathWeb

The dark pink marked roads indicate that these routes have been mapped for road information, including IRI data. An unmarked road indicates no data were collected.

The PathWeb application provides the road surface plan view (Figure 20) and the driver view (Figure 21) when the road data were collected.
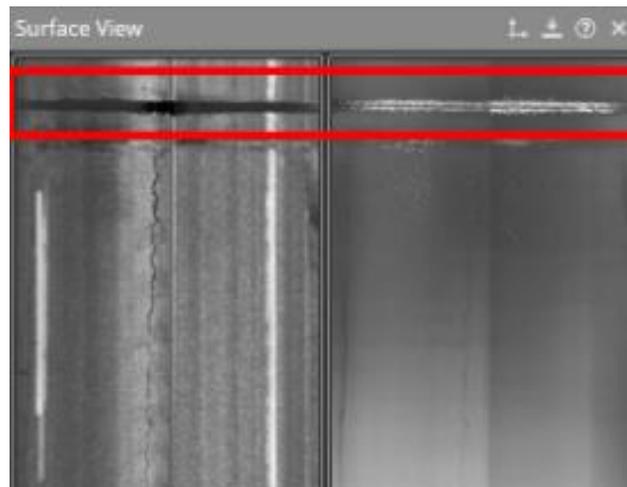
Figure 20. Road surface at bridge entrance expansion joint

Figure 21. Bridge 6485.3L030 entrance view

From these views, the research team was able to identify the bridge deck approach and the traffic lane in which the IRI data were collected. This allowed the research team to obtain the desired data and ensure that the IRI data were collected from the same travel lane as that used for field testing.

Once the bridge location and bridge approach and driver lane were identified, an IRI graph was generated, as shown in Figure 22.
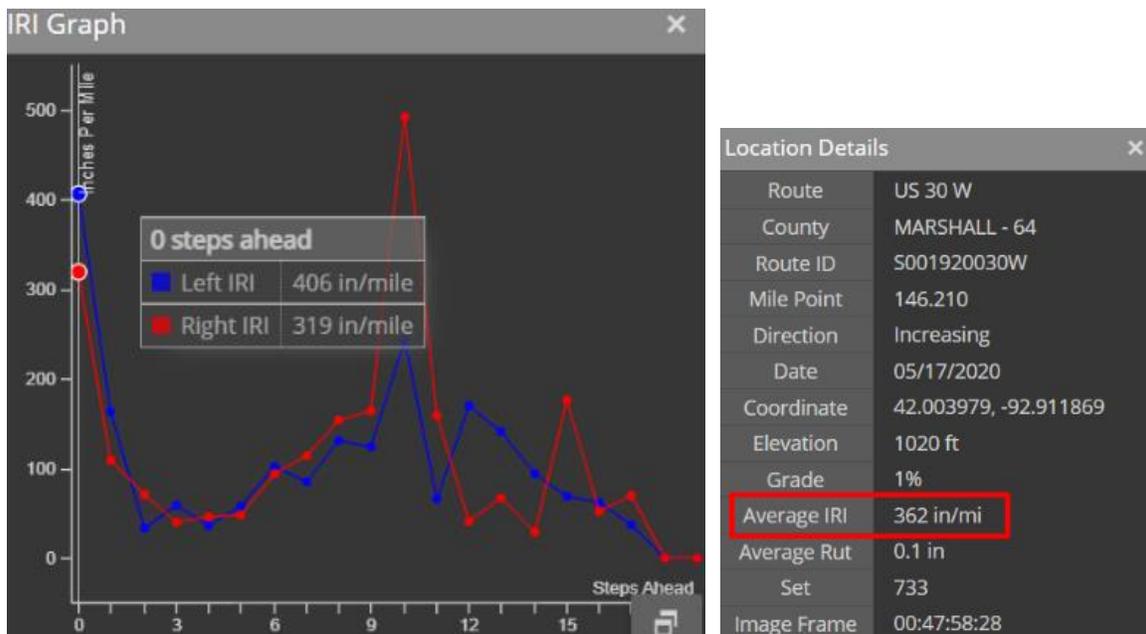
Figure 22. IRI data extraction from PathWeb for bridge 6485.3L030

Note that PathWeb has two IRI data sets: one recorded in each vehicle wheel line.

4.2 IRI Data Extraction

Based on the results from the first phase of this research (Deng and Phares 2016), the deck surface condition near the approach appears to be important to the bridge dynamic response under live loads. In recognition of this, the IRI data were extracted from four locations near the deck approach as listed below with the designations used hereafter:

- After entry – On the bridge between 40 ft and 80 ft from the expansion joint
- Entry – On the bridge between 0 ft and 40 ft from the expansion joint
- 1st point – On the approaching slab between 0 ft and 40 ft before the expansion joint
- 2nd point – On the approaching slab between 40 ft and 80 ft before the expansion joint

Figure 23 illustrates the four locations from which the IRI data were extracted.
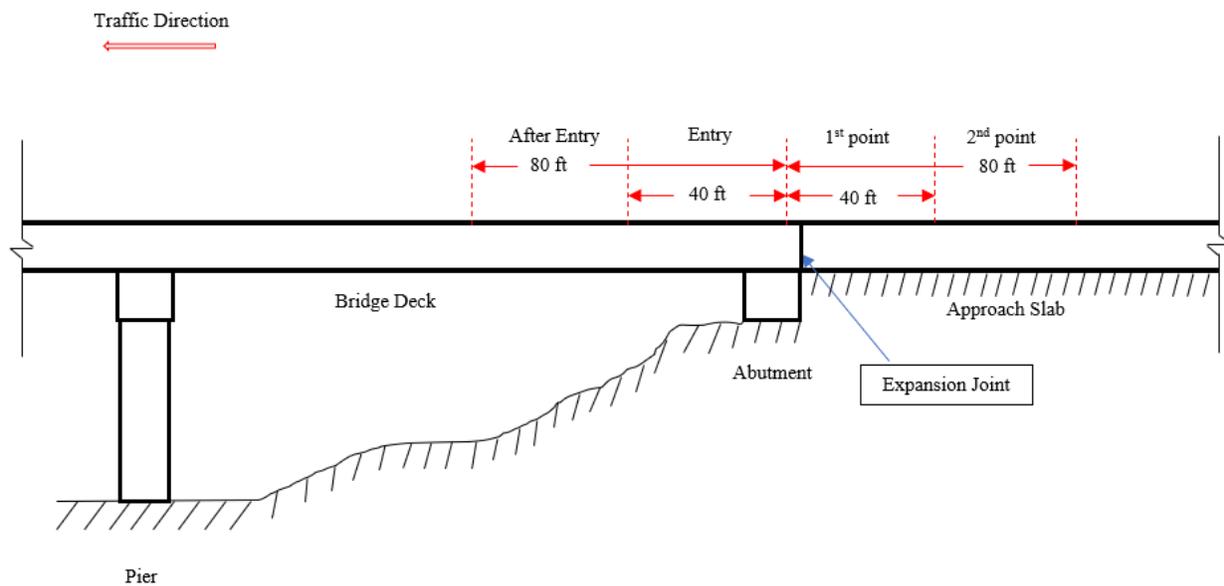
Figure 23. Schematic explanation of After entry, Entry, 1st point, and 2nd point

The actual location of the IRI data collection point varied for each bridge depending on data availability.

4.3 Correlation between DIF and IRI

The main objective of this research was to identify a relationship between the DIF and IRI values, which could eventually be used to estimate the impact factors for all existing bridges during the bridge rating process. To achieve an accurate correlation, the IRI data from the traffic lane that a truck traveled during the field test were extracted and used.

During the DIF data calculation, the researchers found that the DIF values for what were classified as empty trucks were widespread. Given the strain induced from these truck events is low, DIF data for empty trucks were filtered out, and only data from non-empty trucks were used in IRI correlations.

Based on the IRI and DIF data availability, the sample size was further reduced to 13. Table 5 shows the IRI data at the 1st point, 2nd point, Entry, and After entry for the final 13 bridges. (See the previous Figure 23 for data extraction locations.)

Table 5. IRI data collected near the bridge deck approach

| | | IRI data (in/mile) | | | | |
| | | | | | | Max IRI |
Bridge ID	Bridge skew	1st point	2nd point	Entry	After entry	(2nd point data excluded)
6485.3L030	0	54	254	362	136	406
7708.5S235	18	116	118	493	154	506
7774.0R065	3	125	219	58	136	145
4045.2R035	7	210	96	234	215	349
5076.6R080	0	49	67	552	210	647
7780.8L065	17	87	406	140	244	284
7788.3L035	45	45	65	178	31	199
8601.1L030	0	167	174	499	90	507
9167.8L065	0	140	266	77	77	160
4045.4R020	0	161	141	160	157	251
4263.4L020	0	581	403	532	360	706
8603.3R030	29	132	65	127	177	199
0831.6R030	0	907	176	107	104	907

For the 1st point, 2nd point, Entry, and After entry IRI data, the average value of the left and right wheel line IRI values was calculated and used. The researchers found that a wide range of IRI data values existed near the bridge deck appoaches. The IRI values for the final 13 bridges ranged from 49 to 907. The researchers also found that, for a particular bridge, the IRI value near the approach location could change dramatically. For example, the IRI values at 2nd point, Entry, and After entry for bridge 0831.6R030 ranged from 104 to 107, while the IRI value at 1st point was 907.

Once the IRI data values were determined, they were analyzed in conjunction with the calculated DIF data values. Figure 24, Figure 25, Figure 26, and Figure 27 plot the calculated DIF versus IRI at 1st point, 2nd point, Entry, and After entry, respectively.
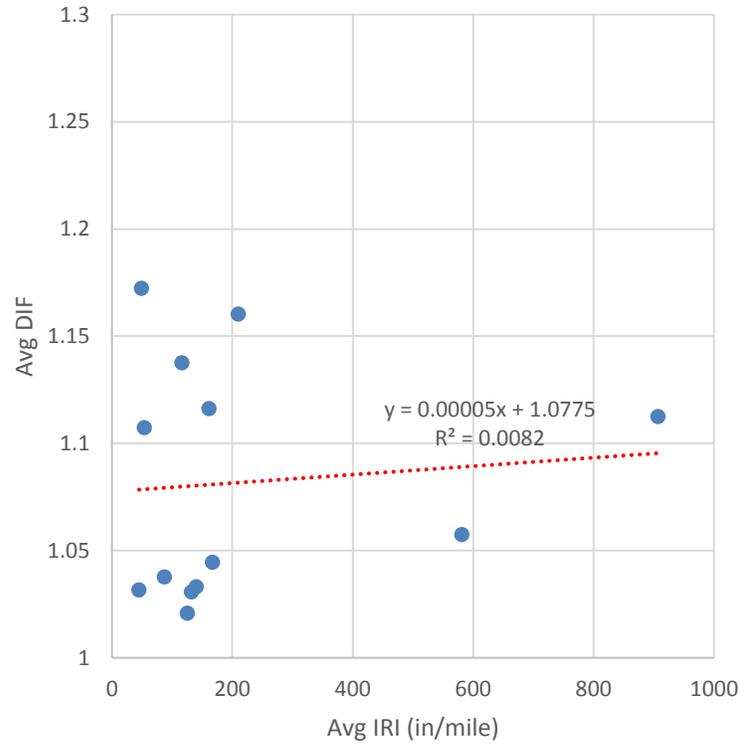

**Figure 24. DIF vs. IRI at 1st point from 13 bridges**
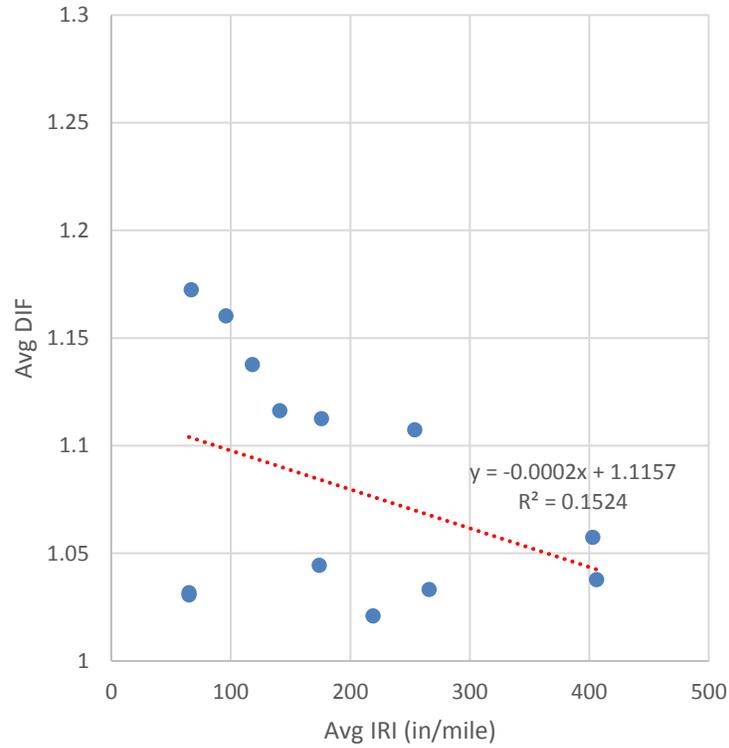
**Figure 25. DIF vs. IRI at 2nd point from 13 bridges**
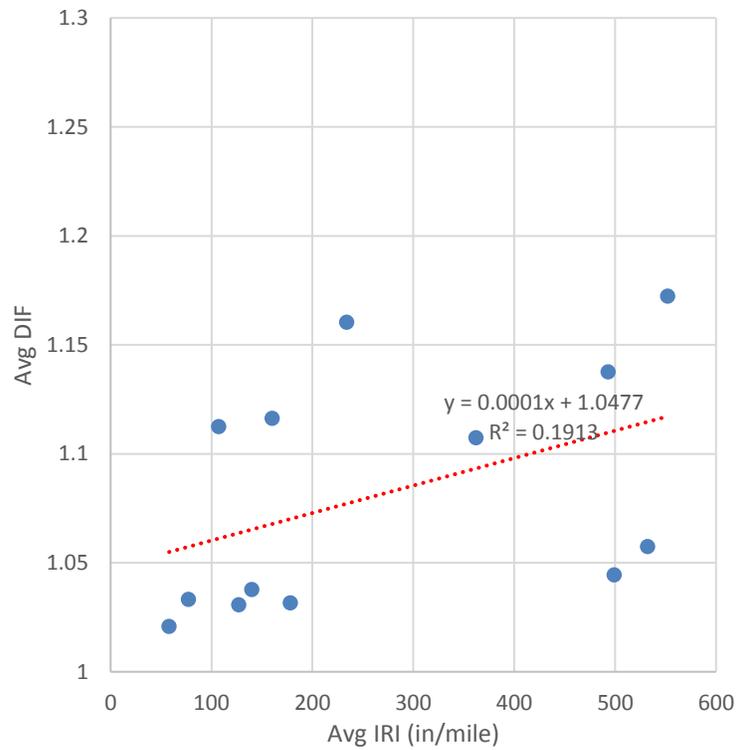
**Figure 26. DIF vs. IRI at Entry from 13 bridges**

37
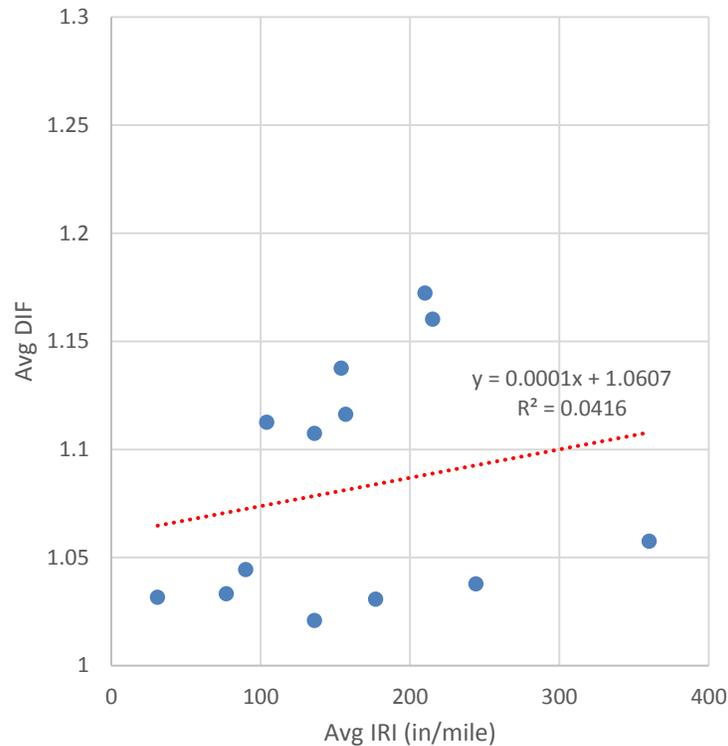
Figure 27. DIF vs. IRI at After entry from 13 bridges

The DIF data in these figures are the (average) DIF induced by one or multiple non-empty truck event(s) for each bridge. Linear regression lines were created in Figure 24, Figure 25, Figure 26, and Figure 27 to reflect the trend of data. In each plot, an R-squared value was generated to show the correlation between the spread data and the regression line. A high R-squared value close to 1.0 indicates a good correlation, and a low R-squared value close to 0.0 indicates a poor correlation.

The results from Figure 24, Figure 25, Figure 26, and Figure 27 indicate that, except for Figure 25 with the IRI data from the 2nd point, the IRI data show a positive relationship to the DIF data; so, when the IRI increases, the DIF increases. This shows agreement with the results from Deng and Phares (2016) and matches the intuition that the rougher surface induces more vertical vibration on the vehicles, resulting in a greater dynamic response on the bridge structure.

As noted, Figure 25 shows the opposite relationship to that shown in the other three figures. This is probably because the IRI data recording location (2nd point) is far from the bridge, and vibration generated by the uneven surface at the 2nd point locations were not reflected in the bridge response.

Given the results indicated that bridge dynamic response is highly related to the bridge surface roughness level (IRI) at 1st point, Entry, and After entry, it could be that the bridge DIF may relate to the roughest location (highest IRI) in these regions. Because of this, the maximum IRI

data at 1st point, Entry, and After entry were extracted and are listed in the last column of the previous Table 5.

Figure 28 was created to correlate the DIF versus maximum IRI at 1st point, Entry, and After entry.
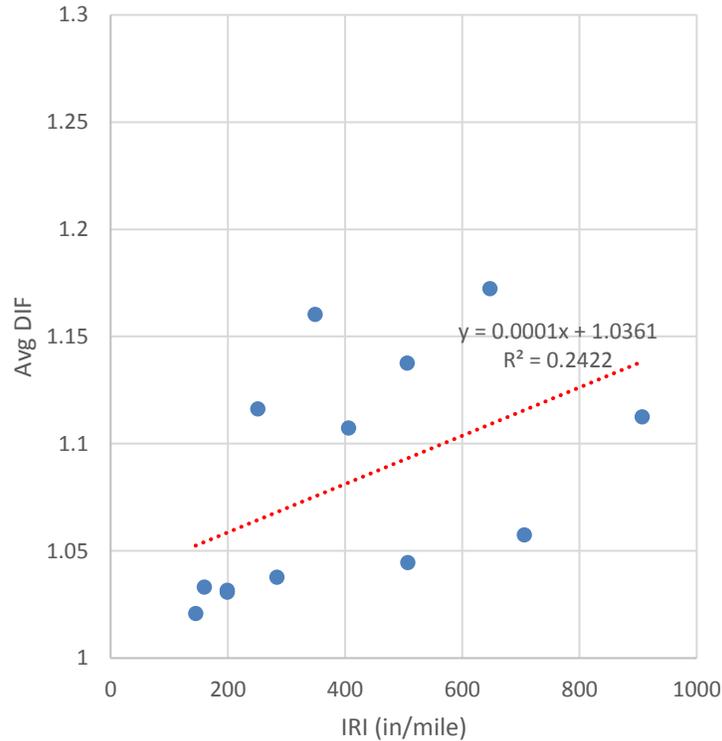
Figure 28. DIF vs. Max. IRI from 13 bridges

Note that the IRI data used in Figure 28 were the raw IRI data without averaging the left and right wheel line values. The slope of the regression line in Figure 28 indicated that the DIF value increases about 0.01 per 100 increments of IRI value.

Given the results from the literature review and Section 3.6 indicated that the bridge skew shows a significant effect on the bridge dynamic response, the data used to establish the relationship between DIF and IRI should exclude the effect of bridge skew. To do that, Figure 29 was plotted with the same approach as Figure 28, but only for the bridges without skew.
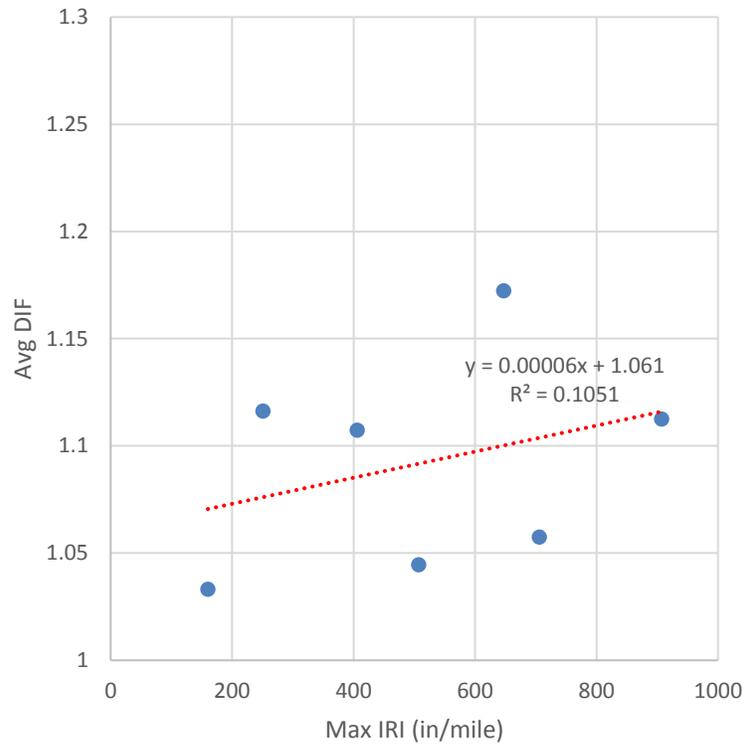
Figure 29. DIF vs. Max. IRI from bridges without skew

The slope of the regression line indicated that the DIF value increased by about 0.006 per 100 in/mile increment of IRI value.

**CHAPTER 5. PROPOSED APPROACH TO DETERMINE BRIDGE DIF**

Given that performing a live load test or instrumenting and monitoring all of the existing bridges to determine their DIFs is not possible, the development of an approach to predict DIF based on the available bridge information was an important project goal. Given the results from the literature review and this research indicate that both bridge skew and bridge surface roughness have a significant effect on the bridge dynamic response, the new approach should include both parameters.

This chapter documents the equation that was developed for the prediction of DIF for existing bridges. The validation of the proposed equation was verified using the field data collected from the 13 monitored bridges.The implementation and limitations of the proposed equation were discussed with the TAC in finalizing this report.

5.1 Development of Equation for Estimation of DIF

Based on the results from Section 4.3, the following equation was developed to correlate the DIF to IRI for bridges without skew.

$$DIF = 1.061 + 0.00006 \times IRI \tag{7}$$

This equation was extracted from the linear regression of the DIF versus IRI data from tested bridges with zero skews. See the previous Figure 29 for details of the bridge data and linear regression.

The results from Section 3.6 indicated that DIF decreases about 0.037 to 0.043 per 10-degree increment of bridge skew. Considering the effect from the bridge skew, a value 0.004/degree within the range was used to account for the bridge skew, and equation (7) was further updated as follows:

$$DIF = 1.061 + 0.00006 \times IRI - 0.004 \times S \tag{8}$$

where S is the bridge skew in degrees. Note that since equation (8) was developed utilizing the maximum IRI data near the bridge deck approach from 40 ft before the bridge to 80 ft on the bridge, the data within the same range should be used during the implementation of this equation for the prediction of the DIF value on other bridges.

5.2 Verification of Proposed Equation

The data from the 13 field-monitored bridges were used to verify equation (8). The predicted DIF values were calculated based on the bridge information, including the bridge skew and the maximum IRI at the bridge deck approach from 40 ft ahead of it to 80 ft on the bridge deck.

Table 6 shows the comparison of the DIF value determined using field-collected strain data and that predicted using equation (8).

Table 6. Verification of proposed equation

| Bridge ID | Bridge skew | Max IRI (in/mile) | DIF data | | Error rate (%) |
			Determined by field-collected strain data	Predicted by equation (8)	
6485.3L030	0	406	1.107	1.094	-1.2
7708.5S235	18	506	1.138	1.028	-9.6
7774.0R065	3	145	1.021	1.067	4.5
4045.2R035	7	349	1.160	1.062	-8.4
5076.6R080	0	647	1.172	1.109	-5.4
7780.8L065	17	284	1.038	1.019	-1.8
7788.3L035	45	199	1.032	1.0	-3.2
8601.1L030	0	507	1.044	1.100	5.4
9167.8L065	0	160	1.033	1.080	4.5
4045.4R020	0	251	1.116	1.085	-2.8
4263.4L020	0	706	1.057	1.112	5.2
8603.3R030	29	199	1.031	1.0	-3.1
0831.6R030	0	907	1.112	1.124	1.1

To evaluate the difference between the field data determined DIF (*Determined DIF*) and the equation (8) predicted DIF (*Predicted DIF*), the difference (error) between the determined and predicted DIF was calculated using equation (9).

$$Error\ rate\ (\%) = \frac{Predicted\ DIF - Determined\ DIF}{Determined\ DIF} \times 100 \qquad \textbf{(9)}$$

The rightmost column in Table 6 shows the results of the difference. The results indicated that the proposed equation (8) shows high accuracy in the prediction of the DIF value given the error rate ranges within ±10%.

Although the proposed equation was validated against the IRI of 13 field-monitored bridges, considering the small sample size, further validation of this equation is still recommended with the data from more bridges.

CHAPTER 6. SUMMARY AND CONCLUSIONS

In some instances, permit vehicles are limited due to anticipated dynamic bridge response exceeding allowable stress levels. As such, it could be advantageous to have bridge-specific dynamic behavior estimates such that permits could be safely issued.

A prior project (Deng and Phares 2016) indicated that the roughness at the entrance to bridges is a primary influence on the general bridge dynamic impact response. The objectives of this project were to correlate IRI data (which are widely collected and directly related to bridge deck roughness) to impact factors and develop a process for determining the impact factor to use for all bridges.

To achieve the project objectives, a sample of 40 bridges having a variety of bridge lengths, skew angles, girder materials, deck conditions, structure types, etc., were identified and verified to be representative of the Iowa bridge population. A smaller sample of 20 bridges was then selected for bridge monitoring to collect dynamic strain data. To estimate the static strain data, the LOWESS function was used to smooth the dynamic strain time history. The DIF value was then calculated using maximum dynamic and static strain data.

IRI data were extracted from PathWeb, a web-based application provided by the Iowa DOT for all bridges considered in the field test program. Once the bridge was identified in PathWeb, the IRI data from four locations near the bridge deck approach were extracted and used to study the relationship between the IRI and the DIF. Based on the results from this research, these were the key findings:

- The DIF decreases as bridge skew angle increases. Based on linear regression, the DIF value decreases about 0.037 to 0.043 per 10-degree increment of bridge skew.
- The DIF decreases as the bridge deck condition index increases, meaning that the dynamic response is lower when the bridge deck condition is better.
- For bridges with zero skew, the DIF vaue increases by 0.006 per 100 in/mile increment of the bridge's IRI value.

Given the research findings, the researchers developed an equation for the prediction of the DIF on existing bridges with consideration of the bridge skew and the maximum IRI value near the bridge deck approach. Although the equation was validated using the data from 13 bridges, the researchers recommend using the equation with the limitation that the actual bridge dynamic response could deviate ±10% from the equation predicted value.

REFERENCES

AASHTO. 2010. *AASHTO Load and Resistance Factor Design (LRFD) Bridge Design Specifications, Customary U.S. Units.* 5th Edition, with 2010 Interim Revisions. American Association of State Highway and Transportation Officials, Washington, DC.

Billing, J. R. and R. Green. 1984. Design Provisions for Dynamic Loading of Highway Bridges. *Transportation Research Record: Journal of the Transportation Research Board*, No. 950, pp. 94–103.

Cantieni, R. 1983. *Dynamic Load Tests on Highway Bridges in Switzerland—60 Years of Experience of EMPA*. Swiss Federal Laboratories for Materials Testing and Research, Dübendorf, Switzerland.

Chang, D. and H. Lee. 1994. Impact Factors for Simple-Span Highway Girder Bridges. *Journal of Structural Engineering*, Vol. 120, No. 3, pp. 704–715.

Cleveland, W. S. 1979. Robust Locally Weighted Regression and Smoothing Scatterplots. *Journal of the American Statistical Association*, Vol. 74, No. 368, pp. 829–836.

Deng, L. and C. S. Cai. 2010. Development of Dynamic Impact Factor for Performance Evaluation of Existing Multi-Girder Concrete Bridges. *Engineering Structures*, Vol. 32, No. 1, pp. 21–31.

Deng, L., Y. Yu, Q. Zou, and C. S. Cai. 2014. State of the Art Review of Dynamic Impact Factors of Highway Bridges. *Journal of Bridge Engineering*, Vol. 20, No. 5.

Deng, Y. and B. Phares. 2016. *Investigation of the Effect of Speed on the Dynamic Impact Factor for Bridges with Different Entrance Conditions*. Bridge Engineering Center, Iowa State University, Ames, IA. https://intrans.iastate.edu/app/uploads/2018/03/dynamic_impact_factor_for_bridge_entrances_w_cvr.pdf.

Li, H. 2005. *Dynamic Response of Highway Bridges Subjected to Heavy Vehicles*. PhD dissertation. Florida A&M University and Florida State University, Tallahassee, FL.

Memory, T. J., D. P. Thambiratnam, and G. H. Brameld. 1995. Free Vibration Analysis if Bridges. *Engineering Structures*, Vol. 17, No. 10, pp. 705–713.

Mohseni, I., A. Ashin, W. Choi, and J. Kang. 2018. Development of Dynamic Impact Factor Expressions for Skewed Composite Concrete-Steel Slab-On-Girder Bridges. *Advances in Materials Science and Engineering*, Vol. 2018, Article ID 4313671, 9 pgs.

National Bridge Inventory (NBI) - Data Dictionary. https://nationalbridges.com/nbiDesc.html. Downloaded June 2022.

PathWeb. https://rams.iowadot.gov/pathweb/. Downloaded February 2022.

Schwarz, M. and J. A. Laman. 2001. Response of Prestressed Concrete I-Girder Bridges to Live Load. *Journal of Bridge Engineering*, Vol. 6, No. 1, pp. 1–8.

SIIMS. https://iowadot.gov/siims. Downloaded October 2021.

THE INSTITUTE FOR TRANSPORTATION IS THE FOCAL POINT FOR TRANSPORTATION AT IOWA STATE UNIVERSITY.

InTrans centers and programs perform transportation research and provide technology transfer services for government agencies and private companies;

InTrans contributes to Iowa State University and the College of Engineering's educational programs for transportation students and provides K–12 outreach; and

InTrans conducts local, regional, and national transportation services and continuing education programs.

INSTITUTE FOR TRANSPORTATION

IOWA STATE UNIVERSITY

Visit **InTrans.iastate.edu** for color pdfs of this and other research reports.